Radiochemical study of the $^{12}C(^3He, ^7Be)$ reaction mechanism at 30 MeV†

A. J. Pape* and S. S. Markowitz
Department of Chemistry and Lawrence Berkeley Laboratory, University of California, Berkeley, California 94720
(Received 7 April 1975)

The excitation function for the $^{12}C(^3He, ^7Be)$ reaction has been measured up to incident energies of 31 MeV, and the ^7Be recoil properties determined in a series of catcher foil experiments at 30 MeV. Based on the different recoil properties of ^7Be formed by each of four different mechanisms, the contribution of each has been estimated. At 30 MeV the predominant mode of ^7Be formation is through sequential decay of the compound nucleus $[^{15}O]^* \rightarrow [^{11}C]^* + \alpha_1 \rightarrow ^7Be + \alpha_2 + \alpha_1$ ($\approx$39 mb). This is followed in importance by the direct n pickup reaction to certain excited states in ^{11}C followed by α-particle emission $[^{11}C]^* \rightarrow ^7Be + \alpha$. The direct α-particle pickup reaction and compound nucleus evaporation of ^7Be have smaller cross sections ($\approx$1 mb and $<$1 mb, respectively).

[NUCLEAR REACTIONS $^{12}C(^3He, ^7Be)$, $E \leq 31$ MeV; measured $\sigma(E, \theta)$; deduced reaction mechanisms.]

I. INTRODUCTION

The excitation function for the $^{12}C(^3He, ^7Be)$ reaction has been measured for ^3He bombarding energies up to 31 MeV. A series of catcher foil experiments was undertaken to elucidate the reaction mechanisms for an incident energy of 30 MeV. The four mechanisms assumed most probable are

(1) $^{12}C + ^3He \rightarrow ^7Be + ^8Be$ (direct α-particle pickup),

(2) $^{12}C + ^3He \rightarrow [^{15}O]^* \rightarrow ^7Be + ^8Be$ [compound nucleus (CN) formation with emission of ^7Be],

(3) $^{12}C + ^3He \rightarrow [^{15}O]^* \rightarrow [^{11}C]^* + \alpha_1 \rightarrow ^7Be + \alpha_2 + \alpha_1$ (CN formation with sequential emission of two α particles),

(4) $^{12}C + ^3He \rightarrow [^{11}C]^* + \alpha_1 \rightarrow ^7Be + \alpha_2 + \alpha_1$ [direct n pickup (or α-particle knockout) followed by α-particle emission].

The ^7Be recoil properties for these four mechanisms are sufficiently different from each other that an estimation can be made of the importance of each. These measurements detect ^7Be recoils over their entire energy range and give information on that predominant ^7Be fraction having energies too low to be studied by counter-telescope methods.

In spite of a certain number of simplifying approximations, it can be shown that the formation of ^7Be at 30 MeV proceeds almost entirely through the two reactions whereby ^7Be is the decay product of an intermediate ^{11}C species. Estimated contributions determined for each of the mechanisms are summarized in Table III at the end of the paper. This work complements another study at approximately the same incident energy in which it was suggested that three particles were involved in the final state.[1]

II. EXPERIMENTAL METHOD

The ^3He beams were obtained at the heavy-ion linear accelerator. The carbon target foils used in the excitation function runs were of approximately 2.5 mg/cm^2 thickness and were fabricated by carbonizing disks of filter paper between graphite bricks. Thinner targets for the recoil experiments were made from a colloidal suspension of graphite. All carbon foils were heated above 1000°C and cooled under vacuum to remove gaseous impurities. The amount of ^7Be arising from the oxygen remaining in the target foils, calculated from the amount of oxygen determined by ^3He activation analyses[2] and the $^{16}O(^3He, ^7Be)$ cross section,[3] was completely negligible compared to the activity formed from the carbon targets. Catcher foils used were commercially available high purity metal foils.

For the excitation function runs, stacked foils were mounted in a Faraday cup target holder with electron suppression. In all experiments in which absolute cross sections were determined, the beam current integrator was calibrated with a standard cell. Following a delay after bombardment to allow shorter-lived nuclides to decay, the ^7Be was detected without interference from other reaction products. The ^7Be was detected by means of its 477 keV γ ray in a calibrated 7.5 × 7.5 cm NaI(Tl) spectrometer.

One type of $^{12}C(^3He, ^7Be)$ recoil experiment utilized a carbon target sandwiched between many nickel, silver, or gold catcher foils. The ^7Be produced in the bombardment of the target re-

coiled into the forward and backward catcher foils. Values of F and B (the fraction of the ^7Be produced which recoils out of the target in the forward and backward directions, respectively) and activity profiles which are the projections of the ^7Be recoil trajectories on the beam axis were obtained. The ^7Be activation in the catcher foils was determined in separate ^3He irradiations of nickel, silver, and gold stacked targets.

The double differential cross section (angular and energy distributions) was obtained in an experiment in which a stack of catcher foils was placed perpendicular to the beam axis and several centimeters downstream from a thin target. Following irradiation, the stack was cut into concentric annuli and counted to obtain the ^7Be angular and energy distributions out to 30° (lab).

In cases where the beam passed through a foil to be counted for its ^7Be content, ^7Be had to be radiochemically separated. Standard chemical procedures were used, finally yielding BeO. The product was determined to be spectroscopically free of the catcher foil element and of all holdback carriers and to be radiochemically pure.

III. RESULTS

The excitation function for the $^{12}C(^3He, ^7Be)$ reaction is shown in Fig. 1. Data are compiled from two runs. The half-life was taken to be 53.6 day [6] and the branching ratio of the 477 keV γ ray to be 0.1038 (Ref. 7). The range-energy (RE) curve for ^3He in carbon was taken from Williamson and Boujot.[8]

Figure 2 presents the results obtained in the

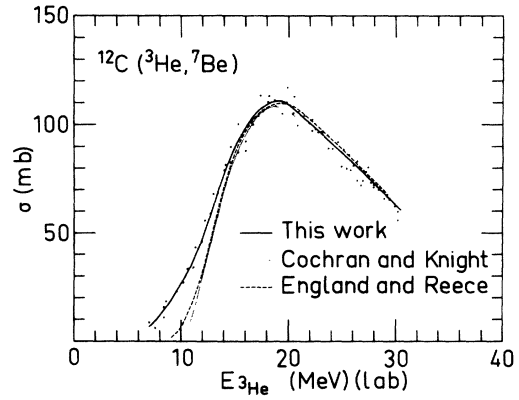

FIG. 1. Excitation function for the $^{12}C(^3He, ^7Be)$ reaction. Data from other sources (Ref. 1 and 4) have been normalized to the ^7Be half-life and branching ratio used in this work. Several data points from Ref. 5 (not shown) in this energy region fall near these curves. (These authors determined the excitation function up to 100 MeV.) Data points (not shown) from Ref. 3 fall well below these curves.

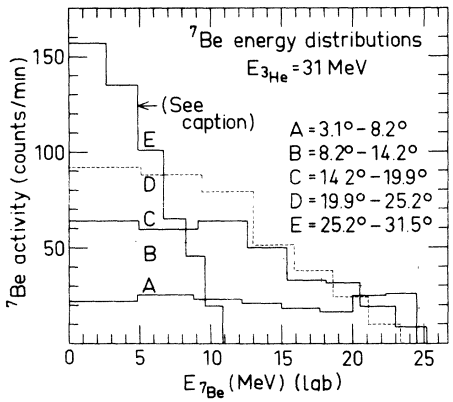

FIG. 2. Laboratory angular and energy distributions for the $^{12}C(^3He, ^7Be)$ reaction for an incident energy of 31 MeV. For the histogram E, the experimental energies were divided by two before plotting.

double differential cross section experiment. Figure 3 shows the data transformed into the center of mass (c.m.) of ^{15}O. The angular distributions for each energy group, as far out as they go in the c.m., appear to be either isotropic (histograms A and B) or composed of forward peaked and isotropic components (histograms C

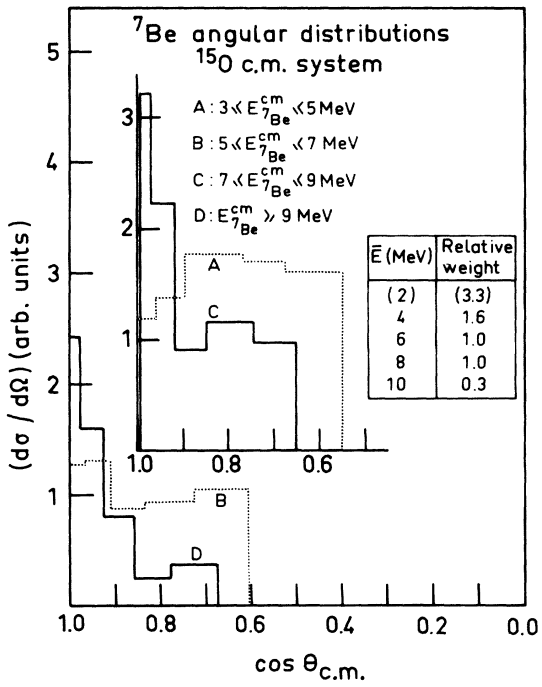

FIG. 3. Data of Fig. 2. transformed into the ^{15}O c.m. system. When the forward-peaked contributions in the histograms C and D are removed, the relative contribution of each assumed isotropic c.m. energy group is that given in the table insert. The contribution of the 2 MeV group was obtained from the experiment of Fig. 4.

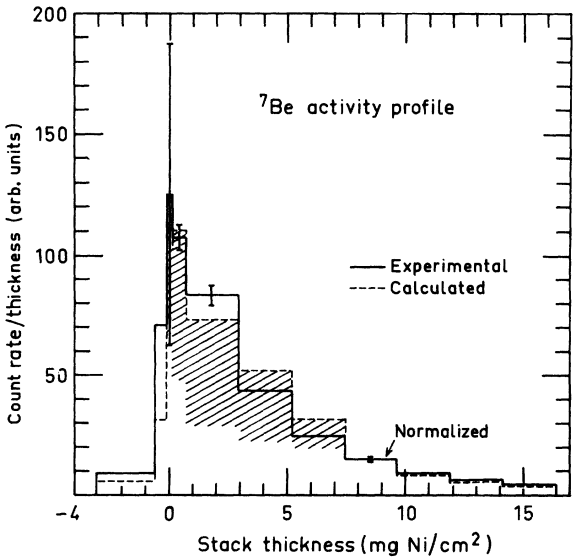

FIG. 4. Experimental and calculated activity profiles for a sandwiched target recoil experiment. The ^{3}He energy at the 120 μg/cm^2 target was 30.4 MeV. The cross-hatched area is the contribution of the 2 MeV c.m. energy group. The small direct part has been included in the last two downstream catcher foils.

and D). Calculations were made on this basis. Forward-backward peaked distributions ($1/\sin\theta$) give activity profiles much too flat to fit the sandwiched target data. Calculations for the recoil experiments followed the general lines given by Winsberg and Alexander.[9]

Figure 4 shows the experimental and calculated activity profiles for a target sandwiched in a stack of nickel catcher foils. For the presentation of the experimental data, the activity in each foil has been divided by the catcher foil thickness. Also, for plotting purposes the carbon target has been converted to an equivalent metal thickness by using the ratio of the stopping powers of carbon and nickel. In this paper all ^{7}Be activities have been normalized to a common time (end of bombardment) and, whenever relevant, have been corrected for chemical yield (approximately 80%) and for the very small ^{7}Be catcher foil activation by the beam during bombardment. The uncertainty in the ^{7}Be activity in each catcher foil of Fig. 4 was taken as ±5%; that of the activity in the target film was taken as ±50%. The large uncertainty is assigned because radiochemical separation of the ^{7}Be from the carbon was not feasible and the presence of other radionuclei (recoils from the catcher foils) caused the ^{7}Be activity determination to be imprecise.

The calculated histogram in Fig. 4 was obtained by using the experimental relative weights of the 4, 6, 8, and 10 MeV c.m. energy groups obtained in Fig. 3, after subtraction of the forward peaked ^{7}Be in the 8 and 10 MeV groups. The relative weight of the 2 MeV group could not be obtained from the experiment of Fig. 2 because of ambiguities in the transformation between the laboratory and c.m. systems. The weighting (3.3 parts in the table insert of Fig. 3) of this assumed isotropic group was taken as that necessary to fill out the downstream activity profile of Fig. 4. The contribution of this group is shown by the cross-hatching in the figure.

In Table I are given the experimental and calculated F and B values for three runs near 30 MeV incident energy. A set of RE curves computed by Altman[10] was used here and in all cases except the double differential cross section experiment. In that run the catcher foil material was aluminum and a ^{7}Be RE curve calculated from the experimental ^{9}Be curve[11] was used. In comparison with existing data, Altman's curves may slightly overestimate the range of a given energy ^{7}Be. Revising his curves in the direction indicated by the available experimental RE information has the effect of bringing the calculated values of F towards the experimental ones.

The calculations of B are not expected to be very accurate because they depend on the assumption that ^{7}Be ranges are proportional to energy in the low energy region where this may not be true. The RE curves used in this work indicate that low energy ^{7}Be (< 2 MeV) has a larger range than given by the relationship $R = kE$, where k is evaluated in the higher energy region (10–20 MeV), where the equation is valid. This causes the calculated values of B to be smaller than the experimental values, as is observed in all cases.

Nuclear collision processes, which can produce

TABLE I. Experimental and calculated F and B values for the ^{12}C(^{3}He, ^{7}Be) reaction at 30 MeV. Calculated values take into account the target thickness.

Target (mg C/cm^2)	$\bar{E}$ (MeV)	F(obs)	F(calc)	B(obs)	B(calc)
0.12	30.4	0.85± 0.03	0.85	0.11 ±0.01	0.06
0.27	30.4	0.76± 0.03	0.79	0.08 ±0.01	0.04
2.48	30.1	0.49± 0.02	0.51	0.011 ±0.001	0.006

appreciable wide angle scattering of very low energy recoils, should not be of importance in the experiments reported here. A similar conclusion was reached by Hower.[12]

IV. DISCUSSION

A. Mechanism 1: Direct α-particle pickup

An interpretation for the energetic forward-peaked ^{7}Be in the 8 and 10 MeV groups (Fig. 3) is that it arises from a direct process. No accompanying peak was observed at 180° in the angular distribution experiments.[1] Considerations of spins, parities, momentum transfer, and the interaction radius involved in the model of such a direct process indicate that it is reasonable to expect a ^{7}Be distribution peaked at 0°. The cross section under the forward peaks in Fig. 3 is approximately 2% of the ^{7}Be formation cross section or ≈ 1 mb.

The energetic ^{7}Be components from the ^{12}C-$(^{3}He,^{7}Be)$ reaction have been studied using counter telescopes for several incident energies around 30 MeV.[13-16] It was observed that the ^{7}Be was generally peaked in the forward direction and that the cross section exhibits an oscillatory behavior with angle. In these studies the integrated direct cross section was ≈ 0.2 mb.

Less detailed recoil experiments have been performed at 15, 20, and 25 MeV. The activity profiles were all qualitatively similar to that given in Fig. 4. There was no evidence for a large contribution from the direct mechanism around 20 MeV as postulated in Ref. 5.

B. Mechanism 2: CN formation with emission of ^{7}Be

At the excitation energies encountered in these experiments, this mechanism would necessarily proceed through the states listed in Table II. In this breakup little ^{7}Be can be formed with c.m. energies between 5 and 7 MeV, whereas a contribution of one part was observed (Fig. 3). No reasonable variation of mechanism 4 (discussed later) will give ^{7}Be in the 5–7 MeV or higher c.m. energy groups. Mechanism 1 is assumed not to contribute to the isotropic components of any of the c.m. energy groups. Any enhancement from the evaporation mechanism for c.m. energies greater than 5 MeV is not visible against the activity arising from mechanism 3 (next section), which gives equal contributions in each c.m. energy interval. The decay channels giving low c.m. energy ^{7}Be would be supressed by the Coulomb barrier between the ^{7}Be particle and ^{8}Be residue.

An upper limit to the evaporation cross section of ^{7}Be from ^{15}O can be estimated from the ^{12}C-$(\alpha,^{7}Be)$ cross section[18,5] at the same nuclear excitation. From statistical model calculations,[19] the $(^{3}He,^{7}Be)$ cross section for evaporation has an upper limit of some tens of μb. In view of the uncertainties in such a calculation and of possible uncertainties in the $(\alpha,^{7}Be)$ cross section, we include a conservative estimation < 1 mb for this evaporation mechanism.

C. Mechanism 3: Sequential emission of two α particles from the CN

For successive α-particle emissions from the ^{15}O CN occurring isotropically and at fixed ener-

TABLE II. States through which the $[^{15}O]^{*} = {}^{7}Be + {}^{8}Be$ step can proceed at a ^{3}He bombarding energy of 30 MeV. The excess excitation energy of the CN is 18.3 MeV. The level schemes for ^{7}Be and ^{8}Be were taken from Ref. 17. For the second and third ^{8}Be states which have appreciable natural widths, the value of $\frac{1}{2}\Gamma$ is included.

^{7}Be state (MeV)	^{8}Be state (MeV)	KE ($^{7}Be + {}^{8}Be$) (MeV, ^{15}O c.m.)	KE (^{7}Be) (MeV, ^{15}O c.m.)
0	0	18.3	9.8
0	2.90 ± 0.8	15.4 ± 0.8	8.2 ± 0.4
0	11.4 ± 3.5	6.9 ± 3.5	3.7 ± 1.9
0	16.63	1.7	0.9
0	16.92	1.4	0.7
0	17.64	0.7	0.4
0	18.15	0.2	0.1
0.43	0	17.9	9.5
0.43	2.90 ± 0.8	15.0 ± 0.8	8.0 ± 0.4
0.43	11.4 ± 3.5	6.5 ± 3.5	3.5 ± 1.9
0.43	16.63	1.2	0.6
0.43	16.92	1.0	0.5
0.43	17.64	0.2	0.1

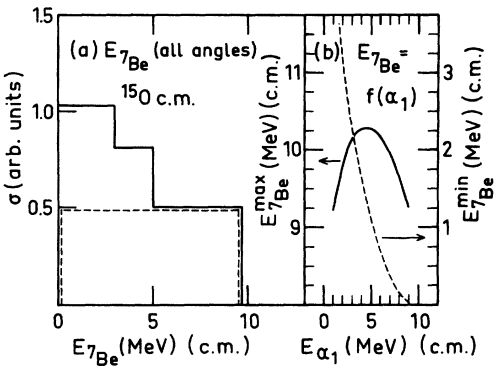

FIG. 5. (a) Histogram showing the relative weights (per MeV) of the c.m. energy groups given in Fig. 3. The dashed histogram represents the contribution of mechanism 3. (b) The variation of the maximum and minimum ^{7}Be energy in the ^{15}O c.m. as a function of the energy of the first emitted α-particle. Energy removed by γ-ray emission is assumed to be negligible.

gies, there results a square ^{7}Be energy distribution in the c.m. (see Appendix). As already mentioned, mechanisms 1 and 2 do not contribute significant isotropic ^{7}Be in the $E>5$ MeV range. Mechanism 4 (next section) makes its principal contribution in the 0–3 MeV range.

Taking an upper cutoff energy of 9.7 MeV for ^{7}Be in the c.m., the square nature of the experimental histogram, in which the cross section per unit energy interval is plotted, is preserved on the high energy side [Fig. 5(a)]. From Fig. 5(b) this corresponds to a low energy cutoff on the square distribution for this mechanism of either 3.3 or 0.2 MeV, with the latter value probably preferred as explained in the next section. The cross section calculated on this basis is 39 mb for this mechanism. This value is still an approximation because in reality the first α particle does not always come off at the same energy.

Calculations have also been made where the first α particle is emitted with an energy spectrum analogous to that observed from heavier nuclei, with the second α particle taking off the remaining excitation energy. Such a model substantially rounds off the square distribution and the fit to the approximately square upper half of the c.m. ^{7}Be energy spectrum is not so good. That the fit is not as good as that for fixed energy α-particle emissions may be because of the low resolution nature of the experiments.

D. Mechanism 4: Direct n pickup (or α-particle knockout) followed by α-particle emission

On the basis of this mechanism, it is necessary that the residual ^{11}C nucleus be left with an excitation of at least 7.5 MeV (binding energy E_B of ^{7}Be in ^{11}C) after the pickup (or knockout). On the other hand, if the ^{11}C excitation is much higher, proton ($E_B=8.7$ MeV) or neutron ($E_B=13.1$ MeV) emission would predominate over ^{7}Be+α breakup. The α particles feeding the ^{11}C ground state and two excited states in the ^{12}C(^{3}He, α)^{11}C reaction at 29 MeV incident energy are forward-peaked and show an oscillatory structure.[20] Pickup data to ^{11}C states higher than 7.5 MeV are not available but even unusual forward-peaked α-particle distributions with subsequent ^{7}Be emission would result in low-energy ^{7}Be that could not recoil out of the cross-hatched part of Fig. 4 (the 2 MeV c.m. group).

TABLE III. Cross section estimates for the ^{12}C(^{3}He, ^{7}Be) reaction mechanisms at 30 MeV incident energy.

Mechanism	(mb)
1. Direct α-particle pickup	≈1
2. $^{12}C+^3He\rightarrow[^{15}O]^*\rightarrow{}^7Be+{}^8Be$	<1
3. $^{12}C+^3He\rightarrow[^{15}O]^*\rightarrow[^{11}C]^*+\alpha_1\rightarrow{}^7Be+\alpha_2+\alpha_1$	≈39
4. $^{12}C+^3He\rightarrow[^{11}C]^*+\alpha_1\rightarrow{}^7Be+\alpha_2+\alpha_1$	≈20
Total ^{7}Be formation cross section	60

When the cross section for this mechanism is taken as that necessary to fill out the low-energy portion of the data after inclusion of the square distribution from mechanism 3, one finds a cross section of either 33 or 20 mb, depending on whether 3.3 or 0.2 MeV is taken as the limit on the square distribution. The smaller value is probably to be preferred because it is in keeping with the trend of a rapidly diminishing neutron pickup cross section per level, on the average, with increasing ^{11}C excitation. This trend is observed for α particles feeding the ground, 4.30, and 4.79 MeV ^{11}C states[20] and is a plausible consequence of the rapidly increasing velocity mismatch between the particles involved in the primary pickup step.

Considering the bombarding energy and the nuclear radii involved, the α-particle knockout is probably not an important reaction mode. However, a contribution from it will give ^{7}Be that will be included in the cross section attributed to mechanism 4, and the importance of mechanism 4 will be overestimated.

For convenience in making the calculations in Sec. III, the 2 MeV group was taken to be isotropic. The assumption of isotropy for the ^{7}Be formed by mechanism 4 is not strictly correct and introduces an additional error in the calculation of the histogram and F and B values. However, there already exists the qualification that the relationship $R=kE$ used does not hold well for low energy ^{7}Be.

The estimated contributions of the mechanisms are summarized in Table III.

We wish to extend our thanks to J. B. England and B. L. Reece for the exchanges concerning their investigation of the $^{12}C(^3He, ^7Be)$ system, and to H. W. Fulbright for discussions on the direct part.

APPENDIX

Here we calculate the ^7Be energy distribution in the ^{15}O c.m. resulting from two successive α-particle emissions from the CN.

In the ^{15}O and ^{11}C reference frames, $p(^{11}C) = p(\alpha_1)$ and $p(^7Be) = p(\alpha_2)$, respectively. With the notation $v(^7Be, \text{c.m. of } ^{15}O) \equiv v_7^{15}$,

$$\vec{v}_7^{15} = \vec{v}_7^{11} + \vec{v}_{11}^{15}$$

or

$$(v_7^{15})^2 = (v_7^{11})^2 + (v_{11}^{15})^2 + (2)(v_7^{11})(v_{11}^{15})\cos\theta \,, \qquad \text{(A1)}$$

where θ is the angle between the vectors. For α-particle emissions at fixed energies from the ^{15}O and ^{11}C progenitors, v_{11}^{15} and v_7^{11} are constants. Multiplying (A1) by $\frac{7}{2}$ to obtain kinetic energy T on the left-hand side and differentiating, one finds

$$dT_7^{15}/d\cos\theta = \text{const.} \qquad \text{(A2)}$$

Letting N represent the number of ^7Be atoms, and substituting (A2) into (A3),

$$dN/dT_7^{15} = (dN/d\cos\theta)(d\cos\theta)/dT_7^{15}) \,, \qquad \text{(A3)}$$

with $dN/(d\cos\theta) = \text{const}$ for isotropic ^7Be emission in the ^{11}C c.m., one obtains

$$dN/dT_7^{15} = \text{const},$$

which is the relationship sought.

---

†This work was supported by the U. S. Atomic Energy Commission.

*Present address: Centre de Recherches Nucleaires, 67037 Strasbourg Cedex, France.

[1]J. B. A. England and B. L. Reece, Nucl. Phys. 72, 449 (1965).

[2]S. S. Markowitz and J. D. Mahony, Anal. Chem. 34, 329 (1962).

[3]T. Mikumo, R. Seki, Y. Tagishi, M. Furukawa, and H. Yamaguchi, Phys. Lett. 23, 586 (1966).

[4]D. R. F. Cochran and J. D. Knight, Phys. Rev. 128, 1281 (1962).

[5]C. B. Fulmer and D. A. Goldberg, Phys. Rev. C 11, 50 (1975).

[6]J. J. Kraushaar, E. D. Wilson, and K. T. Bainbridge, Phys. Rev. 90, 610 (1953).

[7]J. G. V. Taylor and J. S. Merritt, Can. J. Phys. 40, 926 (1962).

[8]C. Williamson and J. P. Boujot, Centre d'Etudes Nucleaires de Saclay Rapport No. CEA-2189, Saclay, France, 1962 (unpublished).

[9]L. Winsberg and J. M. Alexander, in *Nuclear Chemistry I*, edited by L. Yaffe (Academic, New York, 1968), p. 340.

[10]L. Altman, Lawrence Berkeley Laboratory (private communication).

[11]C. O. Hower, Jr., and A. W. Fairhall, Phys. Rev. 128, 1163 (1962).

[12]C. O. Hower, Jr., Ph.D. thesis, University of Washington, Seattle, 1962 (unpublished).

[13]B. Zeidman and H. T. Fortune, Bull. Am. Phys. Soc. 14, 507 (1969).

[14]H. T. Fortune and B. Zeidman, in *Nuclear Reactions Induced by Heavy Ions*, edited by R. Bock and W. R. Hering (North-Holland, Amsterdam, 1970), p. 307.

[15]C. Detraz, H. H. Duhm, H. Hafner, and H. Yoshida, in *Nuclear Reactions Induced by Heavy Ions* (see Ref. 14), p. 319.

[16]G. Audi, C. Detraz, M. Langevin, and F. Pougheon, Nucl. Phys. A237, 300 (1975).

[17]T. Lauritsen and F. Ajzenberg-Selove, Nucl. Phys. 78, 1 (1966).

[18]A. J. Pape, Lawrence Berkeley Laboratory Report No. UCRL-11598 (unpublished).

[19]A. Zucker and K. S. Toth, *Nuclear Chemistry I*, edited by L. Yaffe, (see Ref. 9), p. 409.

[20]J. Catala, A. Garcia, and G. Pardo, An. Fis. Quim. 58A, 267 (1962).